AJNR

Single-voxel proton MR spectroscopy of nonneoplastic brain lesions suggestive of a neoplasm.

H G Krouwer, T A Kim, S D Rand, R W Prost, V M Haughton, K C Ho, S S Jaradeh, G A Meyer, K A Blindauer, J F Cusick, G L Morris and P R Walsh

AJNR Am J Neuroradiol 1998, 19 (9) 1695-1703
http://www.ajnr.org/content/19/9/1695

AJNR Am J Neuroradiol 19:1695–1703, October 1998

Single-Voxel Proton MR Spectroscopy of Nonneoplastic Brain Lesions Suggestive of a Neoplasm

Hendrikus G. J. Krouwer, Thomas A. Kim, Scott D. Rand, Robert W. Prost, Victor M. Haughton, Khang-Cheng Ho, Safwan S. Jaradeh, Glenn A. Meyer, Karen A. Blindauer, Joseph F. Cusick, George L. Morris, and Patrick R. Walsh

BACKGROUND AND PURPOSE: **MR spectroscopy is used to characterize biochemical components of normal and abnormal brain tissue. We sought to evaluate common histologic findings in a diverse group of nonneoplastic diseases in patients with in vivo MR spectroscopic profiles suggestive of a CNS neoplasm.**

METHODS: **During a 2-year period, 241 patients with suspected neoplastic CNS lesions detected on MR images were studied with MR spectroscopy. Of these, five patients with a nonneoplastic diagnosis were identified retrospectively; a sixth patient without tissue diagnosis was added. MR spectroscopic findings consistent with a neoplasm included elevated choline and decreased *N*-acetylaspartate and creatine, with or without detectable mobile lipid and lactate peaks.**

RESULTS: **The histologic specimens in all five patients for whom tissue diagnoses were available showed significant WBC infiltrates, with both interstitial and perivascular accumulations of lymphocytes, macrophages, histiocytes, and (in one case) plasma cells. Reactive astrogliosis was also prominent in most tissue samples. This cellular immune response was an integral component of the underlying disorder in these patients, including fulminant demyelination in two patients, human herpesvirus 6 encephalitis in one patient, organizing hematoma from a small arteriovenous malformation in one patient, and inflammatory pseudotumor in one patient. Although no histologic data were available in the sixth patient, neoplasm was considered unlikely on the basis of ongoing clinical and neuroradiologic improvement without specific therapy.**

CONCLUSION: **Nonneoplastic disease processes in the CNS may elicit a reactive proliferation of cellular elements of the immune system and of glial tissue that is associated with MR spectroscopic profiles indistinguishable from CNS neoplasms with current in vivo MR spectroscopic techniques. Such false-positive findings substantiate the need for histologic examination of tissue as the standard of reference for the diagnosis of intracranial mass lesions.**

Proton MR spectroscopy is a noninvasive technique used to obtain a biochemical profile of brain tissue. Its use as a diagnostic tool in neurooncology both to characterize newly detected intracranial mass lesions (1, 2) and to differentiate recurrent/progressive tumor from radiation-induced necrosis has been reported (3). Typical MR spectroscopic findings in brain neoplasms include the following: a decrease in *N*-acetylaspartate (NAA), a marker of neuronal well-being; an increase in choline (Cho)-containing components involved in increased cell membrane and myelin turnover; and a decrease in creatine (Cr) and phosphocreatine, which provide inorganic phosphates for adenosine triphosphate production.

Recently, single-voxel proton MR spectroscopy, performed at 0.5 T, has shown a high degree of diagnostic accuracy in the differentiation of neoplastic from nonneoplastic tissue has been found (4). Four nonblinded readers (ie, provided with clinical information and previous imaging studies) were able to distinguish neoplastic from nonneoplastic spectra

Received October 3, 1997; accepted after revision May 6, 1998.
Presented in part at the annual meeting of the American Society of Neuroradiology, Toronto, Canada, May 1997.

From the Departments of Neurology (H.G.J.K., S.S.J., K.A.B., G.L.M.), Radiology (T.A.K., S.D.R., R.W.P., V.M.H.), Pathology/Section of Neuropathology (K.-C.H.), and Neurosurgery (G.A.M., J.F.C., P.R.W.), Medical College of Wisconsin, Milwaukee.

Address reprint requests to Hendrikus G. J. Krouwer, MD, Department of Neurology, Neuro-Oncology Service, Medical College of Wisconsin, 9200 W Wisconsin Ave, Milwaukee, WI 53226.

in 54 patients, with a sensitivity of 0.95, a specificity of 1.00, and an accuracy of 0.96. In 35 untreated patients, and with the readers blinded, these values were 0.88, 0.80, and 0.86, respectively. In 13 patients who had undergone forms of treatment (surgery, radiation therapy, chemotherapy, or a combination), these values decreased further (0.79, 0.25, and 0.74, respectively).

We believe that the false-positive and false-negative results of this new test need further investigation. With the growing application of MR spectroscopy as a tool for noninvasive evaluation of intracranial lesions, it is increasingly important that both radiologists and referring clinicians become aware of the pitfalls of this new technique. Whereas false-negative results may cause undue delay of the correct diagnosis and treatment, false-positive results (ie, the presence of a nonneoplastic lesion where a neoplasm was thought to exist) may lead to unnecessary, expensive, and potentially hazardous diagnostic procedures and therapeutic interventions.

We evaluated a subset of false-positive cases with the common histologic finding of a prominent WBC infiltrate and varying degrees of astrogliosis in order to describe the diversity of nonneoplastic processes in these patients.

Methods

Between June 1994 and August 1996, 241 patients with suspected neoplastic brain lesions or recurrent tumors revealed on CT or MR imaging studies underwent MR spectroscopy at our institution. Final diagnoses were available in 106 patients. Nonneoplastic histopathologic findings and neoplastic MR spectroscopic profiles were contradictory in seven of the patients studied during this time span. In five of the nonneoplastic lesions, a prominent WBC infiltrate was found. These five patients, and an additional patient without a tissue diagnosis, form the basis for this report. One patient with an ischemic infarction of undetermined age was not included, because, in retrospect, the MR spectrum was interpreted erroneously.

The medical records of the six patients were reviewed. Clinical information included sex, age, presenting symptoms and neurologic findings, laboratory data (including CSF), final diagnosis, treatment, and outcome. The results of the histopathologic examinations were reviewed with specific attention to WBC infiltrates.

All MR imaging studies were performed on a conventional 0.5- or 1.5-T system. Axial T1-weighted, proton density–weighted, and T2-weighted spin-echo images and contrast-enhanced T1-weighted spin-echo images were routinely obtained.

MR spectra were acquired on a clinical 0.5-T system with a prototype quadrature receive/transmit head coil or a receive-only conformal surface coil (5). The point-resolved spectroscopy (PRESS) pulse sequence was used with chemical-shift selective saturation (CHESS) water suppression, with imaging parameters of 1500/41 (TR/TE) and conventional postprocessing techniques (5). Additional spectra with a TE of 272 were obtained in some cases in which mobile lipid resonances obscured metabolites in the range of 0.5 to 1.5 ppm. Cubic or nearly cubic MR spectroscopic voxels were centered over solid portions of the lesions to avoid necrotic debris with metabolically inactive tissue or edema. A compromise between partial volume effects with large voxels and poor signal-to-noise ratio with small voxels determined a typical voxel size of 1 to 3 cm^3 (MR spectroscopy was not performed for lesions less than approximately 1 cm^3 in size). Regions that showed enhancement on previous studies with IV gadolinium complexes were sampled whenever possible. Localizer images and spectra were typically acquired within 45 minutes. Resonances were assigned as follows: mobile lipids, 0.5 to 1.5 ppm; lactate doublet (Lac), 1.15 ppm and 1.50 ppm; NAA, 2.02 ppm; the combination of glutamine and glutamate (Glx), 2.35 to 2.46 ppm; Cr, 3.04 ppm; Cho, 3.21 ppm; and *myo*-inositol, 3.54 ppm. Spectra were interpreted by visual inspection (4) as being compatible with a neoplastic or nonneoplastic process.

Results

Clinical Data

Five patients were identified whose clinical history and findings at neurologic examination, MR imaging, and MR spectroscopy were suggestive of a neoplasm, yet their final histopathologic diagnoses were nonneoplastic. One patient fulfilled the description above but no tissue diagnosis had been obtained. His clinical course, however, essentially ruled out the presence of a neoplasm.

The clinical findings are summarized in Table 1. Symptoms and signs at presentation were generally compatible with a wide range of disorders and, therefore, nonspecific. In two patients (cases 1 and 2), a demyelinating disorder had previously (10 months and 7 months, respectively) been diagnosed by means of tissue examination from foci other than those that subsequently yielded a neoplastic MR spectroscopic profile. Another patient (case 5) had been found to have a left cerebellar lesion 19 months earlier, but no tissue diagnosis had been obtained at that time. He improved clinically on an empirical regimen of antibiotics and corticosteroids until his admission at our medical center.

Preoperative CSF analysis was not available in cases 1 and 4. A normal protein level was seen in case 3 (40 mg/dL), and mildly to moderately elevated protein levels (68 to 126 mg/dL) were found in cases 2, 5, and 6. Pleocytosis (40/mm^3, predominantly lymphocytes) was found only in case 3. The CSF immunoglobulin G index was repeatedly normal in all four patients (cases 2, 3, 5, and 6). One oligoclonal band was found in case 2 in one CSF sample. CSF cultures (viral, bacterial, fungal) were all negative, and cytologic findings were nonmalignant in all four cases.

Follow-up data were available for all patients. One patient (case 1) died after refusal of further immunomodulatory treatment as a consequence of rapidly progressive demyelination. The other patient (case 2) with both central and peripheral nervous system demyelination initially deteriorated, despite successive treatments with corticosteroids, IV gamma globulin, plasma exchange, and cladribine. He has recently improved on IV cyclophosphamide therapy but is still unable to walk without assistance, almost 3 years after admission. Two patients (cases 5 and 6) have minor residual neurologic deficits (gait ataxia and clumsiness in case 5, and facial numbness and gait ataxia in case 6). The remaining two patients (cases 3 and 4) have fully recovered and are neurologically intact.

TABLE 1: Clinical findings

Case	Age (y)/ Sex	Symptoms	Signs	Dx	Type of Surgery: Histopathologic Findings	Adjuvant Tx	Status at Follow-up
1	24/M	Focal seizures, right-sided weakness (face, arm, leg)	Dysarthria, right-sided hemiparesis	Demyelinating disease	Autopsy: extensive destruction of myelin throughout L hemisphere, mesencephalon, pons, medulla oblongata, and spinal cord; extensive infiltration by lipid-laden macrophages, prominent perivascular chronic inflammation; relative preservation of axons	Declined	Dead, 6 weeks after admission and 10 months after initial presentation
2	59/M	Blurred vision, unsteady gait	R homonymous hemianopsia, nystagmus, facial palsy R, dysarthria, and dysmetria L	Demyelinating disease	Biopsy: demyelination, reactive gliosis, infiltrates of foamy lipid-laden macrophages and mononuclear cells	Corticosteroids; intravenous gamma globulin; plasma exchange; cladribine; cyclophosphamide	Alive, initial deterioration, presently bedridden but stable, after 3 y
3	18/M	Complex partial seizures	Normal	Chronic viral encephalitis (HHV-6)	Subtotal resection: perivascular and interstitial infiltrates of lymphocytes and mononuclear cells, foci of reactive astrocytes	None	Alive, seizure-free on carbamazepine, after 2.5 y
4	52/M	Focal seizures, right-sided weakness (face, hand)	Dysphasia, hemiparesis R (face, arm, leg), hyperreflexia, Babinski R, and dysmetria R	Small arteriovenous malformation with organizing hematoma	Gross total resection: numerous thin-walled capillary vessels, marked amount of hemosiderin and biliverdin, numerous macrophages; gliosis	None	Alive, seizure-free on valproic acid, after 2.4 y
5	30/M	Headaches, unsteady gait	Gait ataxia, L dysmetria	Inflammatory pseudotumor	Biopsy: perivascular infiltrates of small, lymphocytelike cells and plasma cells	Corticosteroids	Alive, minimal gait ataxia, after 3 years
6	55/M	Vertigo, unsteady gait	L appendicular ataxia, R dysesthesias (face, arm, trunk)	NA	NA	Corticosteroids	Alive, facial numbness and gait ataxia, after 2.8 years

Note.—Dx indicates diagnosis; Tx, treatment; HHV-6, human herpesvirus 6; NA, not available.

Both are seizure-free on a regimen of carbamazepine and valproic acid, respectively.

Neuropathologic Findings

The histopathologic findings are presented in Table 1. The primary disorders diagnosed in five of the six patients were quite variable: fulminant demyelination in cases 1 and 2, chronic viral encephalitis in case 3, a small arteriovenous malformation with organizing hematoma in case 4, and inflammatory pseudotumor in case 5. However, the lesions shared a common finding of an extensive inflammatory cell infiltrate, either interstitial, perivascular, or both. The infiltrates were composed of numerous macrophages, lymphocytes, and monocytes. In addition, reactive astrocytosis was present in most tissue samples.

Imaging Findings

With the exception of case 4, the lesions were characterized as hypointense on precontrast T1-weighted images, hyperintense on T2-weighted images, and hyperintense on proton density–weighted images (Table 2 and Figs 1A–6C). Enhancement after intravenous administration of contrast material was seen at the site of MR spectroscopic sampling in five of the six cases. Three lesions showed various degrees of mass effect.

MR spectroscopic findings established reduced or absent NAA resonances and elevated Cho peaks in all six patients. Cr was decreased or absent in four patients and normal in two. Lipid and/or Lac peaks were elevated in five cases.

Discussion

MR spectroscopy is being used with increasing frequency in patients with neurologic symptoms and signs and imaging studies compatible with a neoplasm (6). As with the introduction of CT and MR techniques, it is hoped MR spectroscopy would provide a characteristic "neoplastic" profile. Such a profile generally is thought to include the following: an attenu-

TABLE 2: Imaging findings

Case	Location	MR Signal (T_1/T_2/PD)	Enhancement	Mass Effect	MRS Data (NAA/Cho/Cr/Lipid, and Lact)
1	L centrum semiovale and corpus callosum	↓/↑/↑	+, peripheral	−	↓/↑/=/↑
2	L parietal lobe and L occipital cortex	↓/↑/↑	+, solid	−	↓/↑/0/↑
3	L mesial temporal lobe	↓/↑/↑	+, solid	+, mild	↓/↑/0/↑
4	L posterior frontal	0/↑/↑	+, peripheral	+	0/↑/0/0
5	L cerebellum	↓/↑/↑	+, solid	+	↓/↑/↓/↑
6	L and R brachium pontis	↓/↑/↑	−, ipsilateral; +, contralateral, peripheral	−	↓/↑/=/↑

Note.—PD indicates proton density–weighted. MR signal: ↓, hypointense relative to gray matter; ↑, hyperintense relative to gray matter; 0, isointense relative to gray matter; +, present; −, absent. MR spectroscopy data: ↓, decreased compared with normal brain; ↑, increased compared with normal brain; =, unchanged compared with normal brain; 0, absent.

ated NAA peak, consistent with neuronal loss; an elevated Cho resonance, indicative of increased turnover (synthesis and/or degradation) of cell membrane and myelin components; an attenuated Cr peak, reflecting depressed cellular energetics; and, in some cases, detectable lipid and Lac peaks, indicating areas of cellular necrosis and anaerobic metabolism, respectively (7). However, it is now known that such an MR spectroscopic profile may be seen in conditions other than neoplasms. Diminished NAA and elevated Cho resonances have been found in healthy neonates (8), in patients with adrenoleukodystrophy (9) and posttraumatic cognitive disorders (10), in liver transplant patients (10), in the subacute phase of global hypoxic-ischemic injury (11), in AIDS patients with progressive multifocal leukoencephalopathy (12), and in the acute inflammatory phase of experimental allergic encephalomyelitis (13). Moreover, differences in the relative amplitudes of NAA, Cho, and other metabolites have also been observed among different cultured cell types, including cerebellar granule neurons, cortical astrocytes, oligodendrocyte-type 2 astrocyte progenitor cells, oligodendrocytes, and meningeal cells (14). These findings indicate that it may not be possible to associate a specific MR spectroscopic profile exclusively with a specific disease process.

The findings of our small series of cases further reveal errors in MR spectroscopy in differentiating nonneoplastic from neoplastic disease when the clinical findings and conventional MR imaging studies were compatible with either one. The common denominator in these lesions was found to be an extensive WBC infiltrate, as well as varying degrees of gliosis. The underlying diseases were variable: fulminant demyelination, subacute to chronic viral encephalitis, organizing hematoma, and inflammatory pseudotumor.

Single large demyelinating lesions in the brain may mimic neoplasms on conventional MR studies (15–18). They may appear as hypointense or inhomogeneous on T1-weighted images, with different patterns of enhancement after contrast administration. Absence of mass effect or edema in the white matter around the lesion, as in two of our patients (cases 1 and 2), may be more characteristic of such demyelinating lesions (15, 18), although these features may be present (17). In more typical cases of multiple sclerosis (both acute and chronic), results of MR spectroscopy have detected modestly reduced NAA and mildly increased Cho peaks (19, 20), but only a few reports contain MR spectroscopic data obtained from these large tumorlike demyelinating lesions. De Stefano and coworkers have reported a decrease in NAA of 70% relative to contralateral normal brain and an increase in Cho by as much as 180% in four patients with such lesions (De Stefano N, Preul M, Matthews PM, Francis GS, Antel JP, Arnold DL, "Metabolic Changes in Acute Demyelinating Plaques Studied Longitudinally by Proton MR Spectroscopic Imaging," presented at the annual meeting of the Society of Magnetic Resonance in Medicine, August 1994). It appears that the application of linear discriminant analysis using the "leaving one out" method may differentiate MR spectra of large demyelinating lesions from those of malignant brain tumors (22).

Infection with human herpesvirus 6 (HHV-6), the causative agent of exanthem subitum (roseola infantum, or sixth disease), is ubiquitous, highly prevalent, and lifelong (23). HHV-6 DNA has been detected by means of polymerase chain reaction in up to 85% of normal brain tissue in adults (24). Reactivation may result in a wide spectrum of clinical manifestations, including a "flulike" illness, pneumonia, encephalitis/encephalopathy, and death (25–27). The occurrence of encephalitis presumably caused by HHV-6, both in immunocompetent (28) and immunocompromised patients (29, 30), has recently been reported, and this virus is currently the focus of research regarding the pathogenesis of multiple sclerosis (31–33).

The MR imaging features of the various herpes encephalitides have been described (34). Herpes simplex type 1 encephalitis generally has prolonged T1- and T2-weighted relaxation in the temporal lobes, insular cortex, subfrontal area, and sometimes the cingulate gyrus, whereas a more diffuse distribution of lesions is characteristic of herpes simplex type 2. Enhancement after injection of contrast material occurs as a late event in both types. Very little experience, however, has been reported with MR imaging of HHV-6 encephalitis. Multiple confluent hyperintense lesions on T2-weighted images in the frontal, parietooccipital and bulbar regions, and periventricular white matter were found in a 31-year-old patient

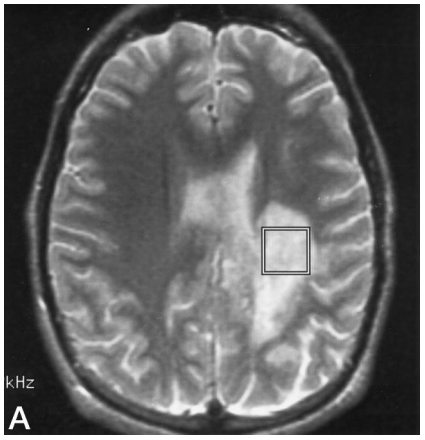

FIG 1. Case 1: 24-year-old man.

A, Axial T2-weighted fast spin-echo (3500/81/1) localizer image for MR spectroscopy shows an infiltrative left centrum semiovale lesion that involved the corpus callosum. Inhomogeneous peripheral enhancement after contrast infusion on T1-weighted images was intense approximately 8 months previously, and faint on the current study (*not shown*).

B, Single-voxel proton MR spectrum obtained at 0.5 T with the PRESS technique (1500/41/256) and CHESS water suppression is compatible with a neoplasm. Resolved peaks in the spectrum are labeled with the corresponding brain metabolite and resonance frequency, expressed in ppm. The elevated Cho resonance amplitude indicates increased membrane turnover (synthesis and degradation), whereas the depressed NAA amplitude reflects neuronal dysfunction or loss. Lactate and mobile lipids indicate increased anaerobic metabolism and cellular necrosis with membrane fragmentation, respectively. At autopsy, the lesion revealed fulminant demyelination with prominent perivascular infiltrates of lymphocytes and macrophages, without evidence of neoplasia.

C, Control MR spectrum obtained from a mixture of left frontal lobe cortex and subcortical white matter in a healthy adult volunteer at 0.5 T with PRESS (1500/41/256) shows an NAA amplitude roughly twice the intensity of Glx, Cr, Cho, and *myo*-inositol (m-Ins). No mobile lipids or lactate are detected.

D, Reference MR spectrum obtained from a brain phantom at 0.5 T with PRESS (1500/41/256) shows a lactate doublet at 1.15 and 1.50 ppm. While the lactate center frequency of 1.33 ppm is independent of the main magnetic field strength, the peaks of the doublet are split further apart at 0.5 T than at 1.5 T (5). Unlike spectra obtained at 1.5 T, individual peaks of the glutamate (and glutamine) multiplet(s) coalesce between 2.2 and 2.4 ppm, because of a collapse of the J-coupling (splitting) that occurs at 0.5 T (5). The phantom contained solutes at the following concentrations and resonant frequencies (±0.05 ppm): Lac (5.0 mmol/L, doublet at 1.15 and 1.50 ppm); NAA (12.5 mmol/L, 2.03 ppm); glutamate (12.5 mmol/L, 2.31 ppm); Cr (10.0 mmol/L, 3.07 ppm); Cho (3.0 mmol/L, 3.21 ppm); and *myo*-inositol (m-Ins) (7.5 mmol/L, 3.57 ppm).

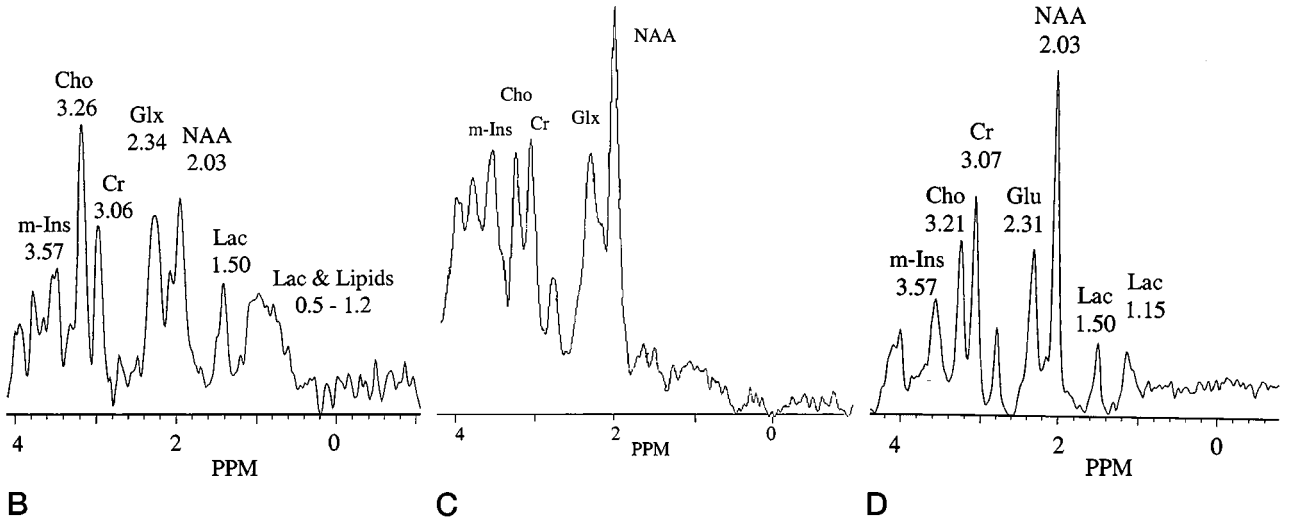

with long-standing multiple sclerosis and an encephalitic episode caused by HHV-6 (33). Small to minuscule areas of hyperintense signal on T2-weighted images in patients with a chronic fatiguelike syndrome and active HHV-6 infection were reported by Buchwald et al (25). However, the authors rightly questioned the significance of these findings regarding an association with HHV-6. A recent report described a fulminant demyelinating encephalomyelitis associated with productive HHV-6 infection in an immunocompetent 21-year-old woman (35). MR findings on T1-weighted images included hypodense concentric lesions without mass effect on the dorsal pons, internal capsule, and parietooccipital lobe, which became hyperintense on T2-weighted images; no enhancement after contrast administration was seen.

MR spectroscopic data regarding herpes simplex encephalitis are also scarce (36–39). They generally document decreased NAA/Cr ratios at various time intervals, interpreted as compatible with neuronal loss. Increased Cho/Cr ratios are thought to reflect myelin breakdown (39) but do not occur in every patient (36). We cannot comment further on the MR spectroscopic findings in our patient, since no such data on acute or chronic HHV-6 lesions are available, to our knowledge.

The final diagnosis in case 4 was a small arteriovenous malformation with organizing hematoma. MR imaging studies in this patient were in retrospect compatible with a hematoma with subacute blood products in the periphery. MR spectroscopic data from an (organizing) hematoma, apart from those obtained from the striatum adjacent to germinal matrix hemorrhages in newborns (40), have not been

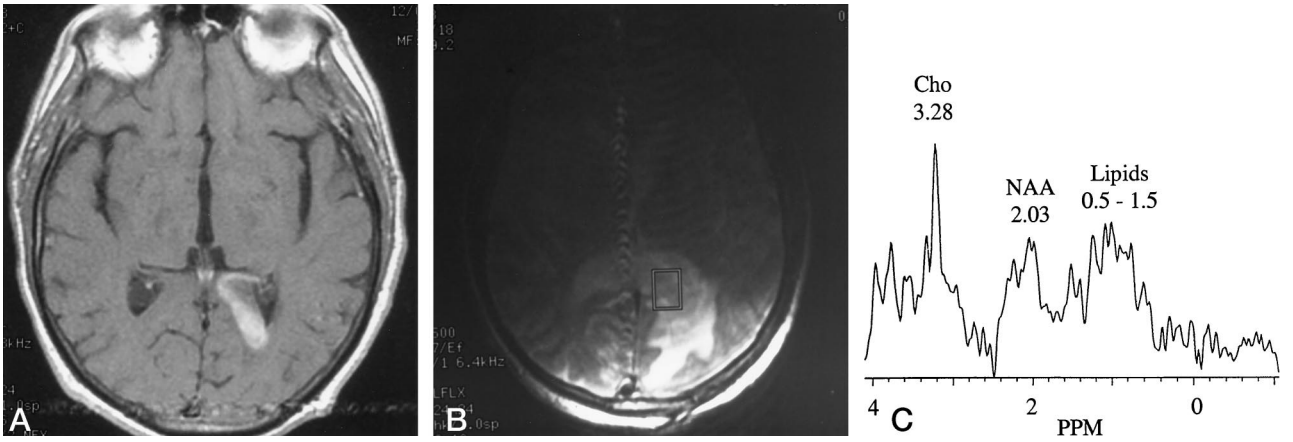

FIG 2. Case 2: 59-year-old man.

A, Contrast-enhanced axial T1-weighted spin-echo (600/20/2) image shows an enhancing mass in the isthmus of the left parietal lobe and occipital cortex.

B, Axial T2-weighted fast spin-echo (2500/87/1) localizer image for MR spectroscopy obtained with a surface coil.

C, MR spectrum (PRESS; 1500/41/256) compatible with neoplasm shows elevated Cho, diminished NAA, and detectable mobile lipid resonances. Neither Glx, Cr, nor *myo*-inositol were detected above the noise floor. Cr serves as a donor of inorganic phosphates for adenosine triphosphate production. Therefore, the absence of Cr reflects depressed cellular energetics. Occipital biopsy revealed demyelination, reactive gliosis, and infiltrates of macrophages and mononuclear cells.

FIG 3. Case 3: 18-year-old man.

A, An axial T1-weighted spin-echo (400/20/2) localizer image obtained with a surface coil shows a left-sided mesial temporal lobe mass. Postcontrast T1-weighted images showed extensive enhancement (*not shown*).

B, MR spectrum (PRESS; 1500/41/256) with a neoplastic profile shows elevated Cho, diminished NAA and Cr, and elevated lactate resonances. Partial temporal lobe resection revealed perivascular and interstitial infiltrates of lymphocytes and mononuclear cells. Subsequent CT-guided biopsy specimen obtained after the lesion enlarged showed similar histopathologic findings. Immunohistochemical studies of the brain tissue sample were positive for human HHV-6.

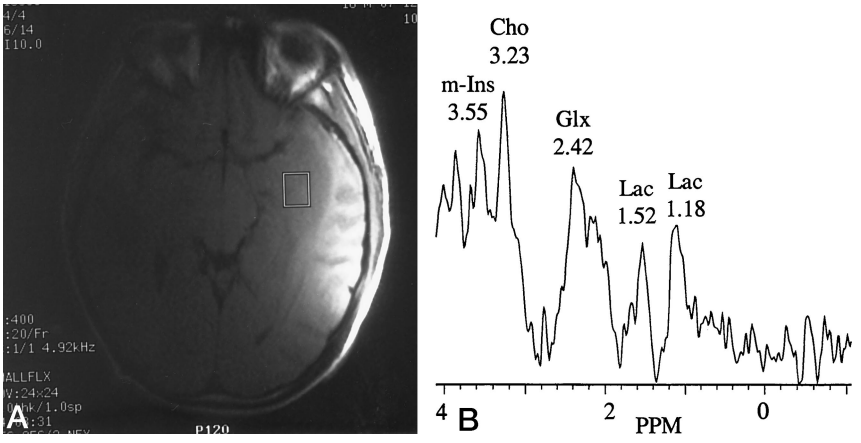

reported, to our knowledge. It is known, however, that hemosiderin-laden macrophages are a characteristic feature of an organizing hematoma (41).

The histopathologic diagnosis in case 5 (inflammatory pseudotumor, also called plasma cell granuloma) is a rare condition. It is characterized by a nonneoplastic proliferation of inflammatory cells, predominantly plasma cells, mixed with variable numbers of lymphocytes, polymorphonuclear leukocytes, mast cells, foamy histocytes, and eosinophils, in a background of fibroblastic stroma with spindle cells (42–44). Its pathogenesis is still unclear, but a viral or bacterial origin has been postulated, as well as an association with previous surgery, trauma, or autoimmune disorders (45). This histopathologic entity occurs most often in the lungs. Many other sites of the body may be involved, including the spleen, liver, gastrointestinal tract, urinary tract, thyroid gland, lymph nodes, skin, orbits, and CNS.

Therapy consists of radical surgical resection, after which close monitoring is recommended. In case of incomplete resection or recurrence of a CNS lesion, radiation therapy or immunosuppressive therapy with corticosteroids has yielded favorable results (43, 44). The prognosis is generally good, with complete radiologic response and survival times up to several years (although reported follow-up periods have been short).

Within the CNS, most inflammatory pseudotumor lesions are dural-based (44, 45). Signal characteristics on MR imaging studies are generally those of hypointensity on T1-weighted images, hyperintensity on T2-weighted images, and homogeneous enhancement after administration of gadolinium complexes. Thus, the preoperative diagnosis of meningioma is most commonly considered. No MR spectroscopic data in patients with inflammatory pseudotumor of the brain have been published because of the rarity of this condition.

Finally, the acute findings and abnormalities on MR images in our sixth patient (case 6) seemed compatible with either demyelinating disease or stroke. CSF findings in this patient, including a slightly elevated protein, a normal immunoglobulin G index, and

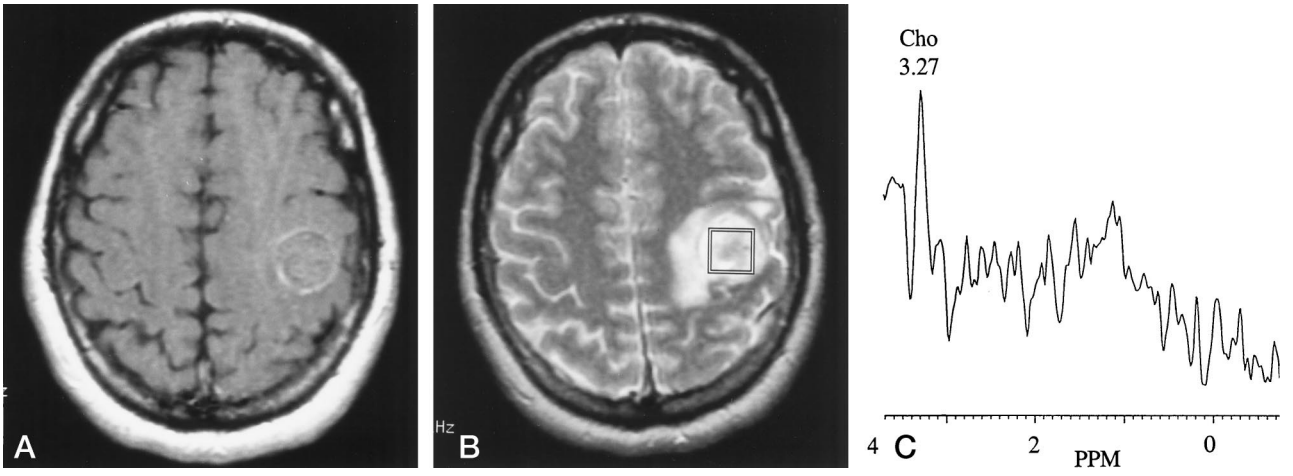

FIG 4. Case 4: 52-year-old man.

A, An axial postcontrast T1-weighted spin-echo (600/25/2) image reveals a mass in the left posterior frontal lobe with faint rim enhancement. Approximately 1 week later, precontrast T1-weighted images showed interval development of subacute blood in the periphery of the lesion (*not shown*).

B, Axial T2-weighted fast spin-echo (3100/81/1) localizer image for MR spectroscopy shows heterogeneous signal intensity within the mass, with surrounding vasogenic edema.

C, MR spectrum (PRESS; 1500/41/256) shows a neoplastic pattern with no detectable metabolites other than Cho. Gross total resection of the lesion showed an organizing hematoma. Results of pathologic examination revealed a small arteriovenous malformation with numerous macrophages. Results of follow-up angiography showed no evidence of an arteriovenous shunt.

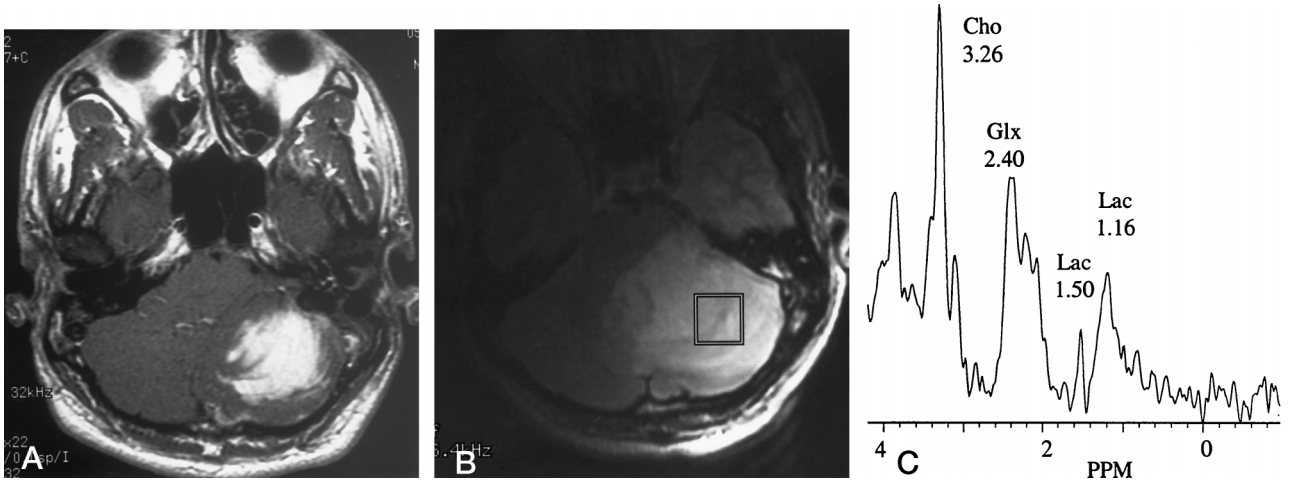

FIG 5. Case 5: 30-year-old man.

A, Axial postcontrast T1-weighted spin-echo (500/20/2) image obtained at 1.5 T shows an enhancing left cerebellar mass with compression of the fourth ventricle. No hemorrhage was noted on precontrast T1-weighted images (*not shown*).

B, Axial T2-weighted fast spin-echo (2500/87/1) localizer image obtained for MR spectroscopy with a surface coil shows hyperintense signal surrounding and within the enhancing region in *A*.

C, MR spectrum (PRESS; 1500/41/256) compatible with neoplasm shows elevated Cho, markedly diminished to absent NAA and Cr, and elevated lactate resonances. A biopsy specimen of the lesion revealed inflammatory pseudotumor, with no evidence of neoplasia.

the absence of oligoclonal bands, may be present in either demyelinating or ischemic conditions. The patient's negative cerebrovascular workup (and because the lesion is not in a classic vascular territory) reduces the likelihood of ischemia and favors demyelination. The patient's clinical course makes a neoplastic process highly unlikely. The patient is still improving, as are his MR imaging studies, without further treatment beyond an initial course of corticosteroids.

The common finding in the patients' histopathologic examinations was the intensive recruitment of cellular components of the immune system as a reaction to the underlying pathophysiological injury. The cellular components were mostly perivascular in location. Some showed mitotic figures. They were, however, not as strongly proliferating and numerous as seen in primary or metastatic CNS lymphoma. Cells in lymphomas usually have more marked atypia and more monoclonal characteristics (46). Regarding immunohistochemistry, CNS lymphomas are usually of the B cell type and far less commonly of the reactive T cell type (46), whereas T cell infiltrate dominated in the lesions in our patients. In demyelinating disease, inflammation, and organizing hematoma, macrophages form an intrinsic component of the immune response. Specific markers (especially HAM-56) are useful in distinguishing neoplastic glial cells from macrophages as part of the immune response in de-

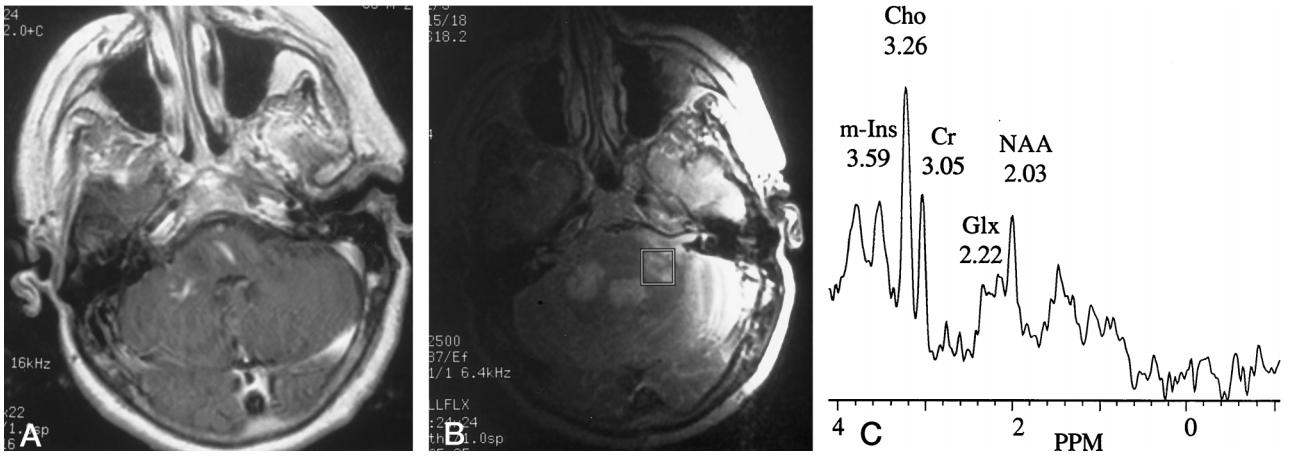

FIG 6. Case 6: 55-year-old man.

A, An axial postcontrast T1-weighted spin-echo (600/20/2) image obtained at 1.5 T shows inhomogeneous enhancement in the right brachium pontis immediately posterior to flow-related artifact. No left-sided enhancement was noted. Precontrast T1-weighted images showed no evidence of hemorrhage in either the left or right middle cerebellar peduncle (*not shown*).

B, Axial T2-weighted fast spin-echo (2500/87/2) localizer image obtained for MR spectroscopy with a surface coil shows hyperintense signal in the brachium pontis on the left and right, with a cursor placed over the left-sided lesion.

C, MR spectrum (PRESS; 1500/41/256) with a neoplastic profile shows elevated Cho and diminished NAA and Glx resonances. No tissue diagnosis has been established, but the patient's clinical course makes neoplasm extremely unlikely.

myelinating disease and hematomas (47). Reactive astrogliosis, common in CNS injury of any kind, was also conspicuous in these lesions. It is now well established that there are intimate interactions between cellular components of the immune system, more specifically microglia, and astrocytes in a number of neurologic disorders. These include demyelination, autoimmune diseases, infections, and neoplasms (48–50). Astrogliosis is the result of astrocytic proliferation, hypertrophy, and increased synthesis of glial fibrillary acidic protein. Cytokines from activated lymphoid cells and microglia are responsible for this increased proliferation of astrocytes (50).

Conclusion

The decreased NAA resonance in the MR spectroscopic profiles of our patients is most likely attributable to the neuron-destroying nature of each lesion, as noted histopathologically. The elevated Cho resonance peaks are compatible with the proliferation of the cellular elements of the immune system and astroglia. The combination of these features mimics the "neoplastic signature" in the MR spectra of these nonneoplastic lesions. MR spectroscopic data compatible with a neoplastic process may thus be found in some lesions that prove to be either inflammatory, demyelinating, or vascular in nature. This new technique should not be considered as a single definitive diagnostic test for final therapeutic decisions in all cases until further experience is reported. Histologic examination of tissue should remain the standard of reference for diagnosis and treatment when clinically indicated and feasible, particularly since some therapies may be detrimental if administered to patients with an erroneous diagnosis (such as radiation therapy administered to patients with demyelinating lesions) (51).

Acknowledgment

We thank Jayne Rossman for manuscript preparation.

References

1. Negendank W, Sauter R, Brown T, et al. **Proton magnetic resonance spectroscopy in patients with glial tumors: a multicenter study.** *J Neurosurg* 1996;84:449–458
2. Preul M, Caramanos Z, Collins D, et al. **Accurate, noninvasive diagnosis of human brain tumors by using proton magnetic resonance spectroscopy.** *Nature Med* 1996;2:323–325
3. Kinoshita K, Tada E, Matsumoto K, Asari S, Ohmoto T, Isoh T. **MR spectroscopy of delayed cerebral radiation in monkeys and humans after brachytherapy.** *AJNR Am J Neuroradiol* 1997;18:1753–1761
4. Rand SD, Prost R, Haughton V, et al. **Accuracy of single-voxel proton MR spectroscopy distinguishing neoplastic from non-neoplastic brain lesions.** *AJNR Am J Neuroradiol* 1997;18:1695–1704
5. Prost RW, Mark L, Mewissen M, Li S-J. **Detection of glutamate/glutamine resonances by magnetic resonance spectroscopy at 0.5 Tesla.** *Magn Reson Med* 1997;37:615–618
6. Castillo M, Kwock L, Mukherji SK. **Clinical applications of proton MR spectroscopy.** *AJNR Am J Neuroradiol* 1996;17:1–15
7. Ott D, Hennig J, Ernst T. **Human brain tumors: assessment with in vivo proton MR spectroscopy.** *Radiology* 1993;186:745–752
8. Toft P, Leth H, Lou HC, Pryds O, Henriksen O. **Metabolite concentrations in the developing brain estimated with proton MR spectroscopy.** *J Magn Reson Imaging* 1994;4:674–680
9. Rajanayagam V, Balthazor M, Shapiro EG, Krivit W, Lockman L, Stillman AE. **Proton MR spectroscopy and neuropsychological testing in adrenoleukodystrophy.** *AJNR Am J Neuroradiol* 1997;18:1909–1914
10. Ross BD, Moats R, Michaelis T, Mandingo JC. **Neurospectroscopy.** In: *Introductory and Advanced MRI: Techniques and Clinical Applications*. Berkeley, CA: Society for Magnetic Resonance in Medicine; 1994:120–126
11. Ross BD, Lee JH, Moats RA. **Clinical MRS for clinical radiologists. In:** *Clinical MR Refresher Course*. Berkeley CA: Society for Magnetic Resonance in Medicine; 1993:109–115
12. Chang L, Ernst T, Tornatore C, et al. **Metabolite abnormalities in progressive multifocal leukoencephalopathy by proton magnetic resonance spectroscopy.** *Neurology* 1997;48:836–845
13. Brenner RE, Munro PMG, Williams SCR, et al. **The proton NMR spectrum in acute EAE: the significance of the change in the Cho:Cr ratio.** *Magn Reson Med* 1993;29:737–745
14. Urenjak J, Williams SR, Gadian DG, Noble M. **Proton nuclear magnetic resonance spectroscopy unambiguously identifies differ-**

ent neural cell types. *J Neurosci* 1993;13:981–989
15. Nesbit G, Forbes G, Scheithauer B, Okazaki H, Rodriguez M. **Multiple sclerosis: histopathologic and MRI and/or CT correlation in 37 cases at biopsy and three cases at autopsy.** *Radiology* 1991; 180:467–474
16. Kepes JJ. **Large focal tumor-like demyelinating lesions of the brain: intermediate entity between multiple sclerosis and acute disseminated encephalomyelitis? A study of 31 patients.** *Ann Neurol* 1993;33:18–27
17. Zagzag D, Miller D, Kleinman G, Abati A, Donnenfeld H, Budzilovich G. **Demyelinating disease versus tumor in surgical neuropathology.** *Am J Surg Pathol* 1993;17:537–545
18. Yetkin Z, Haughton VM. **Atypical demyelinating lesions in patients with multiple sclerosis.** *Neuroradiology* 1995;37:284–286
19. Roser W, Hagberg G, Mader I, et al. **Proton MRS of gadolinium-enhancing MS plaques and metabolic changes in normal-appearing white matter.** *Magn Reson Med* 1995;33:811–817
20. Arnold DL, Matthews PM, Francis G, Antel J. **Proton magnetic resonance spectroscopy of human brain in vivo in the evaluation of multiple sclerosis: assessment of the load of disease.** *Magn Reson Med* 1990;14:154–159
21. De Stefano N, Matthews PM, Antel JP, Preul M, Francis G, Arnold DL. **Chemical pathology of acute demyelinating lesions and its correlation with disability.** *Ann Neurol* 1995;38:901–909
22. De Stefano N, Preul M, Carcamanos I, Francis GS, Antel JP, Arnold DL. **Differentiation between brain tumors and giant demyelinating lesions in vivo using proton magnetic resonance spectroscopic imaging (abstr).** *Neurology* 1997;48:A361
23. Agut H. **Puzzles concerning the pathogenicity of human herpesvirus 6.** *N Engl J Med* 1993;329:203–204
24. Luppi M, Barozzi P, Maiorana A, Marasca R, Torelli G. **Human herpesvirus 6 infection in normal human brain tissue.** *J Infect Dis* 1994;169:943–944
25. Buchwald D, Cheney P, Peterson D, et al. **A chronic illness characterized by fatigue, neurologic and immunologic disorders, and active human herpesvirus type 6 infection.** *Ann Intern Med* 1992; 116:103–113
26. Suga S, Yoshikawa T, Asano Y, et al. **Clinical and virological analyses of 21 infants with exanthem subitum (roseola infantum) and central nervous system complications.** *Ann Neurol* 1993;33: 597–603
27. McCullers JA, Lakeman F, Whitley R. **Human herpesvirus 6 is associated with focal encephalitis.** *Clin Infect Dis* 1995;21:571–576
28. Moschettini D, Balestri P, Fois A, Valensin P. **Acute encephalitis due to human herpesvirus 6.** *Clin Infect Dis* 1996;23:397–398
29. Drobyski W, Knox K, Majewski D, Carrigan D. **Brief report: fatal encephalitis due to variant B human herpesvirus-6 infection in a bone marrow-transplant recipient.** *N Engl J Med* 1994;330:1356–1360
30. Knox K, Harrington D, Carrigan D. **Fulminant human herpesvirus six encephalitis in a human immunodeficiency virus-infected infant.** *J Med Virol* 1995;45:288–292
31. Sola P, Merelli E, Marasca R, et al. **Human herpesvirus 6 and multiple sclerosis: survey of anti HHV-6 antibodies by immunofluorescence analysis and of viral sequences by polymerase chain reaction.** *J Neurol Neurosurg Psychiatry* 1993;56:917–919
32. Carrigan DR, Harrington D, Knox KK. **Subacute leukoencephalitis caused by CNS infection with human herpesvirus-6 manifesting as acute multiple sclerosis.** *Neurology* 1996;47:145–148
33. Merelli E, Sola P, Barozzi P, Torelli G. **An encephalitic episode in a multiple sclerosis patient with human herpesvirus 6 latent infection.** *J Neurol Sci* 1996;137:42–46
34. Jordan J, Enzmann D. **Encephalitis.** *Neuroimaging Clin N Am* 1991;1:17–38
35. Novoa LJ, Nagra RM, Nakawatase T, Edwards-Lee T, Tourtellotte WW, Cornford ME. **Fulminant demyelinating encephalomyelitis associated with productive HHV-6 infection in an immunocompetent adult.** *J Med Virol* 1997;52:301–308
36. Takanashi J, Sugita K, Ishii M, Aoyagi M, Niimi H. **Longitudinal MR imaging and proton MR spectroscopy in herpes simplex encephalitis.** *J Neurol Sci* 1997;149:99–102
37. Demaerel PH, Wilims G, Robberecht W, et al. **MRI of herpes simplex encephalitis.** *Neuroradiology* 1992;34:490–493
38. Menon DK, Sargentoni J, Peden CJ, et al. **Proton MR spectroscopy in herpes simplex encephalitis: assessment of neuronal loss.** *J Comput Assist Tomogr* 1990;14:449–452
39. Hitosugi M, Ichijo M, Matsuoka Y, Takenaka N, Fujii H. **Proton MR spectroscopy findings in herpes simplex encephalitis.** *Clin Neurol* 1996;36:839–843
40. Toft PB, Leth H, Peitersen B, Lou HC. **Metabolic changes in the striatum after germinal matrix hemorrhage in the preterm infant.** *Pediatr Res* 1997;41:309–316
41. Davis RL, Robertson DM. ***Textbook of Neuropathology***. Baltimore: Williams & Wilkins; 1985:608–616
42. Hsiang J, Moorhouse D, Barba D. **Multiple plasma cell granulomas of the central nervous system: case report.** *Neurosurgery* 1994; 35:744–747
43. Le Marc'hadour P, Fransen P, Labat-Moleur F, Passagia JG, Pasquier B. **Intracranial plasma cell granuloma: a report of four cases.** *Surg Neurol* 1994;42:481–488
44. Tresser N, Rolf C, Cohen M. **Plasma cell granulomas of the brain: pediatric case presentation and review of the literature.** *Childs Nerv Syst* 1996;12:52–57
45. Al-Sarraj S, Wasserberg J, Bartlett R, Bridges L. **Inflammatory pseudotumour of the central nervous system: clinicopathological study of one case and review of the literature.** *Br J Neurosurg* 1995;9:57–66
46. Burger PC, Scheithauer BW. ***Tumors of the Central Nervous System***. Washington, DC: Armed Forces Institute of Pathology; 1995:321–329; Third Series, Fascicle 10
47. Hulette C, Downey B, Burger P. **Macrophage markers in diagnostic neuropathology.** *Am J Surg Pathol* 1992;16:493–499
48. Giulian D. **Microglia and neuronal dysfunction.** In: Kettenmann H, Ransom BR, eds. *Neuroglia*. New York: Oxford University Press; 1995:671–684
49. Wekerle H. **Antigen presentation by central nervous system glia.** In: Kettenmann H, Ransom BR, eds. *Neuroglia*. New York: Oxford University Press; 1995:685–699
50. Benveniste E. **Cytokine production.** In: Kettenmann H, Ransom BR, eds. *Neuroglia*. New York: Oxford University Press; 1995:700–713
51. Peterson K, Rosenblum MK, Powers JM, et al. **Effect of brain irradiation on demyelinating lesions.** *Neurology* 1993;43:1205–1212